Soil & Environmental Health 3 (2025) 100129

Contents lists available at ScienceDirect

Soil & Environmental Health

journal homepage: www.sciencedirect.com/journal/soil-and-environmental-health

Research Paper

Zinc and cadmium release from soil aggregate of different size fractions during repeated phytoextraction with *Sedum plumbizincicola*: Insight from stable isotope analysis

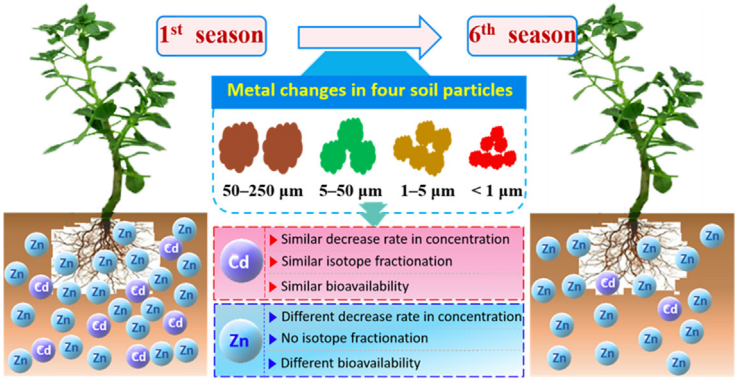
Jiawen Zhou [a], Jingqi Dong [b], Rebekah E.T. Moore [c], Mark Rehkämper [c], Katharina Kreissig [c], Barry Coles [c], Ting Gao [a], Peter Christie [a], Longhua Wu [a,*]

[a] Institute of Soil Science, Chinese Academy of Sciences, Nanjing 211135, China
[b] Center for Soil Protection and Landscape Design, Chinese Academy of Environmental Planning, Beijing 100041, China
[c] Department of Earth Science & Engineering, Imperial College London, London SW7 2AZ, United Kingdom

HIGHLIGHTS

- Similar decrease in Cd concentration in soil aggregate of different size fractions.
- Similar mechanism in Cd uptake from soil aggregate of different size fractions.
- Zn exchange among soil aggregate of different size fractions during phytoextraction.
- Negligible Zn isotope fractionation was found in aggregate of different size fractions.

GRAPHICAL ABSTRACT



ARTICLE INFO

Handling Editor: Lena Q. Ma
Technical Editor: Maria Manzoor

Keywords:
Isotope fractionation
Zn/Cd hyperaccumulator
Plant bioavailability
Long-term phytoremediation
Rayleigh model
Biogeochemical behaviors
Root exudates
Chemical fractionation
Soil acidification
Cation exchange

ABSTRACT

Studies based on metal isotope changes at micro-scale interfaces within soils (i.e., between aggregates of different size fractions) can provide further insight into soil-plant interactions during long-term phytoextraction. Here, aggregate size separation was conducted on two contaminated soils that underwent phytoextraction using Zn/Cd hyperaccumulator *Sedum plumbizincicola* over six consecutive seasons. The dynamic changes in Zn and Cd concentrations, chemical fractionations and isotope compositions in soil aggregates were investigated. As phytoextraction proceeded from the first (C1) to the sixth (C6) season, shoot Zn displayed a marginally heavier isotope composition despite the essentially constant Zn isotope composition of bulk soils and the 50–250, 5–50, 1–5, and <1 μm aggregate size fractions. Most likely, this results from moderate depletion of Zn in the bulk soils (by ≤ 21%) and gradual release of heavy Zn isotopes into soil bioavailable pool due to soil acidification and Zn exchange during repeated phytoextraction. Light isotopes of Cd were significantly enriched in all aggregates of different size fractions ($\Delta^{114/110}Cd_{C6-C1} = -0.14 \pm 0.04$ to -0.02 ± 0.04‰) with similar decreases in Cd concentrations (50–64% and 87–92% in two soils) over the five consecutive seasons. Rayleigh modelling produced similar Cd isotope fractionation factors for aggregates of different size fractions, indicating that similar mechanisms controlled Cd release from soil aggregates. In contrast to other plants preferring light Cd isotopes, Zn/Cd

* Corresponding author.
E-mail addresses: jwzhou@issas.ac.cn (J. Zhou), lhwu@issas.ac.cn (L. Wu).

https://doi.org/10.1016/j.seh.2025.100129
Received 15 October 2024; Received in revised form 9 January 2025; Accepted 9 January 2025
Available online 11 January 2025
2949-9194/© 2025 The Authors. Published by Elsevier B.V. on behalf of Zhejiang University and Zhejiang University Press Co., Ltd. This is an open access article under the CC BY license (http://creativecommons.org/licenses/by/4.0/).

hyperaccumulator continuously took up heavier Cd isotopes from soils. The results were due to the enhanced root exudation to mobilize more Cd from soil solids and organic ligands excreted from roots preferentially complexed heavy Cd isotopes based on density functional theory. The different isotopic behaviours of Zn and Cd suggest different processes controlling their migration in the soil-plant system.

1. Introduction

Excessive accumulation of metals such as Zn and Cd in soils, particularly in the vicinity of mining and smelting areas, is a major concern and represents a high threat to public health (Zhao et al., 2015; Shi et al., 2023). A number of engineering and agricultural options have been developed to remediate metal-contaminated soil. Phytoextraction using hyperaccumulator plants is an *in-situ* and environmentally friendly remediation technique suitable for cleaning up large areas of contaminated agricultural soils (Wu et al., 2013; Sheoran et al., 2016).

Despite the capacity of hyperaccumulators to take up metals from soils, phytoextraction using these plants still requires continuous cropping and long periods of field effort to achieve the remediation target, particularly for highly-contaminated soils (Koopmans et al., 2008; Li et al., 2014a,b). In contrast to short-term experiments with only one or two cropping cycles, soil-available metal concentration could decrease substantially during long-term phytoextraction, thus enhancing the interactions between soil and plants, leading to dynamic re-equilibration of soil-available metal (Huynh et al., 2010; Li et al., 2016; Suo et al., 2021). It is therefore necessary to elucidate the dynamic geochemical processes that underpin Zn and Cd changes in the soil-plant system over long-term remediation periods.

Metal distribution, mobility and availability in soils are largely determined by soil physicochemical properties, such as pH, texture, and the contents of organic matter and Fe/Mn oxides (Zeng et al., 2011; Lamb et al., 2016; Riaz et al., 2021). However, the effect of soil aggregate size distribution is often neglected when adopting strategies to improve phytoextraction performance. Soil aggregate size plays an important role in influencing metal availability in soils and their interaction with plant roots (Huang et al., 2020). Soil aggregates of different sizes differ in mineral and organic components, whereby the larger aggregates (2–2000 μm) are composed mainly of primary minerals such as feldspar and quartz whilst smaller aggregates (< 2 μm) are enriched in phyllosilicate clays, Fe/Mn oxides, carbonates, and organic matter (Luo et al., 2011). Compared to coarser aggregates, finer aggregates show higher affinities to and greater enrichment of Zn and Cd, due to their higher contents of clay minerals, Fe/Mn oxides and organic matter (Quenea et al., 2009; Liu et al., 2010). As a consequence, Zn or Cd is more resistant to release from the finer aggregates into soil solutions and hence accessible to plant roots (Dabkowska-Naskret, 2003; Banerjee et al., 2017; Li et al., 2019). However, the smaller aggregates can also enhance plant uptake of Zn and Cd due to their high specific surface area that provides greater root-particle contact (Chen et al., 2008). Moreover, higher Zn or Cd concentration in the finer aggregates indicates that more Zn or Cd can be potentially supplied from the solid phase to the bioavailable pool to keep up with plant uptake compared to coarser aggregates during long-term phytoextraction. Therefore, studies of metal interactions with soil aggregates of different sizes can give additional information on the mechanisms of micro-scale changes in metal distributions in soil-plant systems.

Conventional analysis of metal concentrations and distributions using different chemical extraction methods provides limited information about metal transformations in soil-plant systems (Li et al., 2016; Gruter et al., 2019). In recent years, metal stable isotope analysis has been widely used to trace metal biogeochemical processes in various environmental matrices, based on the finding that distinct and specific metal isotope fractionations may occur during different biogeochemical processes (Zhong et al., 2020; Wiggenhauser et al., 2022). Wiggenhauser et al. (2021) studying Cd transfer in contaminated soil-rice systems found that a larger fraction of Cd was bound to sulfur during soil flooding than in non-flooded conditions. Consequently, rice plants grown in the flooded soils were enriched in heavier Cd isotopes ($\delta^{114/110}Cd = -0.39$ to -0.37%) relative to those grown in the non-flooded soils ($\delta^{114/110}Cd = -0.56$ to -0.45%), due to the preferential precipitation of light Cd isotopes into Cd sulfides. However, there are few published studies of metal isotope fractionation at micro-scale environmental interfaces such as soil aggregates. Zhu et al. (2018) observed that the $\delta^{114/110}Cd$ values of secondary minerals, which are generated during the oxidative weathering of sulfide phases, increased with decreasing mineral particle size. Their explanation for this is that sulfide minerals preferentially released heavy Cd isotopes into the oxidative fluids and thus the finer clay minerals with higher specific surface tended to adsorb more heavy Cd isotopes from the fluid phase. Regarding soil-plant systems, the distribution of Zn and Cd isotopes in the soil aggregates that are influenced by plant activities are expected to be more complex.

In our previous studies (Zhou et al., 2020, 2024), we showed that Cd isotope compositions varied in aggregates of different size fractions and heavy Cd isotopes were preferentially taken up by the plants from bulk soils over the long-term phytoextraction period. This led to the further question of whether and how Zn and Cd isotopes are further fractionated in soil aggregates on the microscopic scale relative to the bulk soils induced by repeated phytoextraction. It is therefore hypothesized that the different mineral compositions and physiochemical properties of soil aggregates of different size fractions lead to different Zn and Cd bioavailability to plant. Hence, plant uptake should vary at soil aggregates of different size fractions and the aggregate size fraction with greater metal removal by plants will present more pronounced isotope fractionation after long-term phytoextraction. The aims were to (1) study dynamic changes in the isotope fractionations of Zn and Cd between soils and plants during a long-term remediation period, (2) investigate the dynamic changes in Zn and Cd concentrations, chemical fractionations and isotope compositions in aggregates of different size fractions during repeated phytoextraction, and (3) link the metal fractionation and isotope data with the underlying mechanisms that govern metal availability and replenishment for soil aggregates of different sizes.

2. Materials and methods

2.1. Repeated phytoextraction pot experiment

Two agricultural soils (Soil 1 and Soil 2) were collected from a mining and smelting site in Hunan province, China, differing in soil pH, organic carbon content (SOC), clay content and metal availability (Table S1). The sampling site has a long mining history of >120 years with large areas of agricultural soils subjected to high metal contamination. Based on a survey in the vicinity of the mining site (<50 km^2) (Li et al., 2012), the Cd concentration range in the farmland soils was 5.49–21.3 mg kg^{-1} (mean value 13.6 mg kg^{-1}). A substantial part of the agricultural soils was abandoned and could not be used directly for agricultural production prior to remediation.

The duration of the entire experiment was nearly four years over six seasons from November 2015 to June 2018 at the Institute of Soil Science, Chinese Academy of Sciences (Fig. S1). Four cuttings of *S. plumbizincicola* were planted in each pot containing 1.5 kg of soil (oven-dried basis). The plants were grown in a greenhouse with an average temperature of 20–30 °C in the daytime and 5–15 °C at night. Soil moisture content in each pot was maintained at ~70% of water holding capacity by daily watering. Fertilizers (0.5 g urea and 0.5 g KH_2PO_4 per pot) were applied one month after the seedlings of a new cropping cycle had been planted. Detailed information on

pot experiment design and management is presented in Section S1 of the Supplementary Materials. After plant growth for 3–4 months, the plant shoots were harvested while the soils were gently broken up with a wood hamper, with most plant roots carefully picked out and homogenized for representative soil sampling. The procedure of soil homogenization between seasons did not significantly change the distribution of soil aggregate size fractions (please refer to the results section 3.1). Soil subsamples were taken before the first, third and sixth seasons for further chemical analysis.

2.2. Soil aggregate fractionation

Soils collected before the first, third and sixth seasons were used for aggregate size separation. Samples from three replicate pots of each soil were randomly selected. Soils were separated into four aggregate of different size fractions using the methods described by Li et al. (2020), namely size fractions 50–250 μm (F1), 5–50 μm (F2), 1–5 μm (F3) and <1 μm (F4). Wet sieving, sedimentation and centrifugation were used to sequentially separate these four aggregate size fractions. Firstly soil (250 μm, 50 g) was ultrasonically dispersed (60 J mL^{-1}) in 1 L deionized water for 10 min and the 50–250 μm size fraction was obtained by filtration through a 50-μm nylon sieve. The remaining suspension was deposited in a high glass beaker at normal gravity and the settling times determined by Stokes' law (1 h and 20 min at 20 °C) were employed to collect the 5–50 μm size fraction. Finally, the 1–5 μm fraction was separated from the < 1 μm aggregates after centrifugation of the siphoned solution during sedimentation at 402×*g* for 5 min. All recovered aggregate size fractions were air-dried at 60 °C, weighed and homogenized for further analysis. As shown in Table S2, the mass recoveries of all aggregate size fractions accounted for >95% of the total soil mass used for aggregate separation. Additionally, water-extractable fraction of Cd and Zn constituted only a minor fraction (<1%) of total metal in the bulk soils. The water-extractable metal loss during wet sieving showed negligible effect on the results of subsequent soil chemical and isotopic analysis.

2.3. Determination of metal concentrations

Bulk soil and soil aggregate samples (~0.1 g) were first digested in closed Teflon vials with 2 mL concentrated HNO_3 (~15.4 M) and 1 mL $HClO_4$ (~12.5 M) by heating at 120 °C for 2 h and at 200 °C for another 4 h on the hotplate. The solutions were then evaporated to remove HNO_3 at 180 °C until the agglomerate and white acid fog was observed. Following this, 1 mL concentrated HNO_3 and 1 mL HF (28 M) were added and the samples were heated at 200 °C until the solutions became clear. Finally, the sample solutions were dried and dissolved in 10 mL 1% (*m/m*) HNO_3 solution for determination of Zn and Cd by inductively coupled plasma-optical emission spectrometry (ICP-OES, Avio 200, Perkin Elmer, Waltham, MA; detection limit 0.01 mg L^{-1}). Replicates, blanks, and the certified soil reference material GBW07405 were included for analytical quality control with average metal recoveries of 92% (Zn) and 108% (Cd).

Plant shoots (~0.2 g) were digested with 6 mL concentrated HNO_3 and 2 mL 30% H_2O_2 at 105 °C for 6 h and used for Zn and Cd determination by atomic adsorption spectrophotometry (AAS, SpectrAA 220FS, Varian, Palo Alto, CA; detection limit 0.05 mg L^{-1}). Multiple determinations of celery reference material GBW10048 yielded acceptable average metal recoveries of 96% for Zn and 99% for Cd.

2.4. Determination of metal fractionation

Three replicates of the bulk soil and aggregate samples during repeated phytoextraction were used for metal fractionation analysis with a modified Tessier sequential extraction method (Tessier et al., 1979). The detailed extraction method was described by Zhou et al. (2020). The sequentially extracted chemical fractions comprised: (1) E1, exchangeable fraction by 1.0 M $MgCl_2$ solution; (2) E2, carbonate-bound fraction by 1 M NaOAc solution (pH 5.0); (3) E3, Fe/Mn oxide-bound fraction by 0.04 M $NH_2OH{\cdot}HCl$ in 25% (*m/v*) HOAc for 6 h in a water bath at 96 °C; (4) E4, organic matter-bound fraction by 0.02 M HNO_3 and 30% (*m/v*) H_2O_2 in a water bath (85 °C) followed with a extraction of 3.2 M NH_4OAc (dissolved in 20% (*v/v*) HNO_3); (5) E5, residual fraction digested by concentrated HCl and HNO_3. Zinc and Cd in the extract solutions were determined by ICP-MS (Nexion, 2000, Perkin Elmer, Waltham, MA; detection limit 0.5 μg L^{-1}). The whole procedure comprising five sequential extraction steps recovered 106% of total Zn and 104% of total Cd in the bulk soils, indicating a robust analytical procedure.

2.5. Determination of metal isotope compositions

Plant and soil sample pairs from the first (high Cd supply), third (medium Cd supply) and sixth (low Cd supply) cropping cycles were chosen to explore the dynamic isotope variations in the soil-plant system. The sample analyses are comprised of the soils prior to the harvesting of the first, third and sixth season (denoted as Soil-C1, Soil-C3 and Soil-C6) and the shoots harvested at the end of the first, third and sixth season (denoted as Shoot-C1, Shoot-C3 and Shoot-C6) (Table S3 and Fig. S1). These were chosen to enable calculation of metal uptake as a fraction of total soil metal concentration, and to determine the degree of isotope fractionation during uptake at different phytoextraction periods.

The isotopic analysis was carried out in the MAGIC Laboratories at the Department of Earth Science & Engineering of Imperial College London, UK. The analytical procedures were comprehensively described in Zhou et al. (2023), with detailed information given in Section S2 of the Supplementary Materials. Blanks, sample replicates and standard reference materials NIST SRM 2710 (soil) and SRM 1570a (spinach leaf) were processed alongside the samples for quality control. The total procedural blank for the isotopic analysis was 2.0–15.0 ng for Zn and less than ~0.2 ng for Cd, equivalent to < 0.1% of the indigenous Zn (>40 μg) and Cd (>200 ng) mass in the samples. Repeated analysis of IRMM-3702 Zn and NIST SRM 3108 Cd solutions during measurement sessions resulted in a reproducibility of ±0.05‰ for $\delta^{66}Zn$ (n = 153) and ±0.06‰ for $\delta^{114/110}Cd$ (2 SD, standard deviation; n = 42). As shown in Table S4, the reference materials (NIST SRM 2710 and 1570a) and secondary standard solutions (London Zn and BAM Cd) provided robust results (Abouchami et al., 2013; Moore et al., 2017, 2020; Liu et al., 2020; Barati et al., 2023).

The Zn and Cd isotope data for shoots harvested in the first season (Shoot-C1) and the bulk soils before the first (Soil-C1) and sixth (Soil-C6) seasons had been measured previously at the University of Science and Technology of China (Zhou et al., 2020) and the results are compared in Table S5. Notably, the metal isotope compositions determined in the two different laboratories were identical within the instrumental analytical uncertainty.

2.6. Calculations, model fitting and statistical analysis

The Zn isotope data measured relative to IRMM-3702 were further corrected for reporting relative to JMC Lyon Zn, according to Archer et al. (2017). The Zn and Cd isotope compositions of the samples are reported in delta notation (‰) relative to the JMC Lyon Zn or the NIST 3108 Cd reference materials:

$$\delta^{66}Zn = \left[\frac{\left(^{66}Zn/^{64}Zn\right)_{sample}}{\left(^{66}Zn/^{64}Zn\right)_{JMC}} - 1\right] \times 1000 \text{ or } \delta^{114/110}Cd = \left[\frac{\left(^{114}Cd/^{110}Cd\right)_{sample}}{\left(^{114}Cd/^{110}Cd\right)_{NIST\ 3108}} - 1\right] \times 1000 \quad \text{Eq (1)}$$

The apparent isotopic fractionation between two components A and B was calculated according to Equation (2):

$$\Delta^{66}Zn_{A\text{-}B} = \delta^{66}Zn_A - \delta^{66}Zn_B \text{ or } \Delta^{114/110}Cd_{A\text{-}B} = \delta^{114/110}Cd_A - \delta^{114/110}Cd_B \quad \text{Eq (2)}$$

The metal isotope compositions of the bulk soils that were composed of four aggregate size fractions were calculated using the mass averaged isotope value of each size fraction:

$$\delta^{66}Zn_{bulk\ soil} = \frac{\sum_i m_i[Zn]_i \delta^{66}Zn_i}{\sum_i m_i[Zn]_i} \text{ or } \delta^{114/110}Cd_{bulk\ soil} = \frac{\sum_i m_i[Cd]_i \delta^{114/110}Cd_i}{\sum_i m_i[Cd]_i} \quad \text{Eq (3)}$$

where m_i, $[Zn]_i$ and $[Cd]_i$ are the mass of aggregate size fraction i and its concentrations of Zn and Cd, respectively; $\delta^{66}Zn_i$ and $\delta^{114/110}Cd_i$ are the Zn and Cd isotope values of size fraction i.

During repeated phytoextraction, the bulk soil and the aggregate of different size fractions were regarded as closed systems in which Cd isotope fractionation was induced by continuous metal uptake by *S. plumbizincicola*. The observed isotope fractionation was hence fitted using a Rayleigh mass balance equation:

$$\delta^{114/110}Cd_{C3\ or\ C6} - \delta^{114/110}Cd_{C1} = \varepsilon_{Cd} \times \ln f_{Cd} \quad \text{Eq (4)}$$

where $\delta^{114/110}Cd_{C3\ or\ C6}$ and $\delta^{114/110}Cd_{C1}$ denote the Cd isotope compositions of the bulk soils or the aggregate size fractions in the third or sixth season, and in the first season, respectively; f_{Cd} represents the mass fraction of Cd remaining in the bulk soils or aggregate size fractions after each phytoextraction step; and ε_{Cd} is the Cd isotope fractionation factor associated with continuous Cd uptake from soil to plant.

The isotopic data are expressed as mean ± 2SE (standard error), with details on the source and expression of the uncertainties provided in the respective data tables or figures. Other results, such as element concentrations, are quoted as mean ± SE. Significant differences were detected using one-way analysis of variance followed by an LSD test at $p < 0.05$, after tests for normal data distribution (Shapiro-Wilk test) and homogeneity of variance (Levene test) were passed. The correlations between different variables were tested using Pearson correlation analysis. Statistical analysis was conducted using the SPSS 21.0 for Windows software package (IBM, Armonk, NY).

3. Results and discussions

3.1. Mass distribution during repeated phytoextraction

As shown in Fig. 1a, as phytoextraction proceeded, the mass fraction of each aggregate size fraction varied slightly. Hence, long-term phytoextraction did not significantly alter the aggregate size mass distribution pattern of both soils ($p > 0.05$, Fig. 1). Plants are known to influence soil aggregation by enmeshing and binding soil particles or breaking down larger aggregates via root penetration (Bacq-Labreuil et al., 2019). However, *S. plumbizincicola* has a shallow and fibrous root system which does not appear to be effective in changing soil aggregate size fractions after six consecutive seasons.

3.2. Zinc changes in the plant-soil system during repeated phytoextraction

Continuous phytoextraction across five seasons significantly decreased the Zn concentrations of Soils 1 and 2 by 21% and 18%, respectively (Table 1). In addition, compared with the situation before phytoextraction, the Zn concentrations of the 5–50 and 1–5 μm size fractions declined by 22–34% and 16–32% after the fifth season (Table 1). The decreases in Zn mass for the 5–50 and 1–5 μm size fractions contributed to 58–65% and 36–41%, respectively, of the total Zn removal from the bulk soils. However, no significant decline in Zn concentrations occurred in the 50–250 and <1 μm size fractions during repeated phytoextraction. The Zn concentration in the 50–250 μm size fraction of Soil 2 even increased by 36% after the second season, indicating extra Zn supply from other aggregate size fractions. Comparing Zn mass variations in the four aggregate size fractions, *S. plumbizincicola* preferentially took up Zn from the 5–50 and 1–5 μm size fractions.

The Tessier sequential extraction results show that Zn in the four aggregates was mainly bound to Fe/Mn oxides, accounting for 57–72% of total Zn (Fig. 2a). With the prolonged period of phytoextraction, the carbonate-, Fe/Mn oxide- and organic matter-bound Zn concentrations gradually decreased but exchangeable Zn concentrations increased markedly in the 5–50 and 1–5 μm size fractions, even though they show an overall decrease in total Zn concentrations (Table S6). The fraction of Fe/Mn oxide-bound Zn in the 5–50 and 1–5 μm size fractions substantially decreased by 30–37% and 26–35% within five cropping cycles, respectively (Fig. 2a–c). The decrease in total Zn concentration in the bulk soils was hence mainly due to the decreasing concentrations of Fe/Mn oxide-bound Zn for these two aggregate size fractions. This indicates that Fe/Mn oxide-bound Zn, especially from the 5–50 and 1–5 μm size fractions, represented the major Zn source and made the greatest contribution to plant uptake. The exchangeable Zn pool is most readily bioavailable for uptake by plants. However, once this pool was depleted by plant roots, Zn from other pools, and predominantly the Zn fraction bound to Fe and Mn oxides, rapidly compensated for this decrease. Here, two highly Zn-contaminated soils were used in the long-term

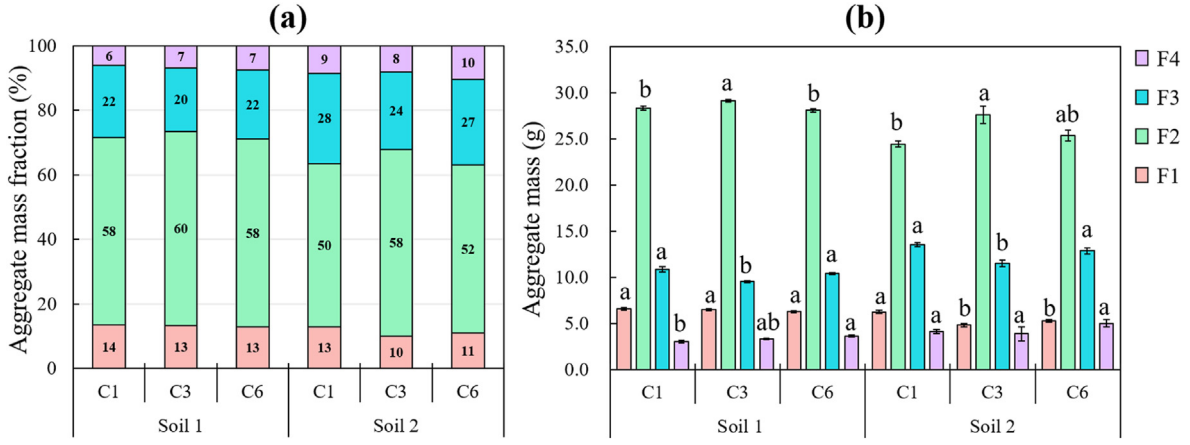


Fig. 1. Soil aggregate mass fractions (a) and mass (b) during repeated phytoextraction. The error bars denote the standard error (SE, $n = 3$). Different lowercase letters for each aggregate size fraction at different phytoextraction periods in the same soil indicate significant differences at $p < 0.05$. C1, C3 and C6, before the first, third and sixth season. F1, 50–250 μm; F2, 5–50 μm; F3, 1–5 μm; F4, <1 μm. Aggregate mass fraction in % = mass of each aggregate size fraction (g)/total mass of all the four size fractions (g) × 100%.

Table 1
Metal concentrations in soil aggregate of different size fractions during repeated phytoextraction (mg kg^{-1}).

Aggregate size fraction	Soil 1						Soil 2					
	Zn			Cd			Zn			Cd		
	C1	C3	C6	C1	C3	C6	C1	C3	C6	C1	C3	C6
Bulk soil	1511 ± 34 a	1471 ± 44 b	1198 ± 5 c	22.3 ± 1.4 a	9.49 ± 0.18 b	2.51 ± 0.14 c	1386 ± 20 a	1355 ± 13 a	1137 ± 17 b	25.2 ± 0.5 a	13.4 ± 0.3 b	5.46 ± 0.13 c
Decrease, %		3	21		57	89		2	18		47	78
F1	1099 ± 28 a	1148 ± 43 a	1027 ± 26 a	25.7 ± 1.9 a	12.9 ± 0.2 b	3.07 ± 0.14 c	525 ± 51 a	716 ± 40 a	661 ± 18 a	21.0 ± 0.9 a	17.8 ± 0.6 a	6.00 ± 0.25 b
Decrease, %		−4	7		50	88		−36	−26		15	72
F2	1367 ± 82 a	1251 ± 10 a	906 ± 15 b	17.6 ± 1.5 a	7.34 ± 0.13 b	2.23 ± 0.04 c	1197 ± 6 a	1146 ± 23 a	931 ± 16 b	17.2 ± 0.7 a	10.8 ± 0.4 b	3.75 ± 0.13 c
Decrease, %		9	34		58	87		4	22		37	78
F3	2312 ± 43 a	2068 ± 17 b	1571 ± 10 c	32.5 ± 3.3 a	11.4 ± 0.2 b	2.59 ± 0.07 c	1882 ± 10 a	1786 ± 21 a	1583 ± 46 b	30.7 ± 1.2 a	17.3 ± 0.7 b	6.21 ± 0.08 c
Decrease, %		11	32		65	92		5	16		44	80
F4	2382 ± 50 a	2204 ± 62 a	2060 ± 69 a	37.7 ± 1.0 a	13.5 ± 0.7 b	3.03 ± 0.26 c	1781 ± 25 a	1779 ± 34 a	1711 ± 24 a	31.5 ± 0.9 a	20.3 ± 1.1 b	6.83 ± 0.31 c
Decrease, %		7	14		64	92		0	4		36	78

Data are expressed as mean ± SE (n = 3). Different lowercase letters indicate significant differences for the same aggregate size fraction at different phytoextraction periods at $p < 0.05$. C1, C3 and C6, before the first, third and sixth season. Soil aggregate size fractions: F1, 50–250 μm; F2, 5–50 μm; F3, 1–5 μm; F4, <1 μm. Metal concentration data before phytoextraction are from our previous study (Zhou et al., 2024). Decrease = (1 – metal concentration after phytoextraction/metal concentration before phytoextraction) × 100%.

phytoextraction experiment. Therefore, the Zn supply from the solid phase to the exchangeable Zn pool was adequate to maintain plant Zn uptake. Moreover, significant soil acidification (pH decreased by 0.35 and 1.64 units in Soil 1 and Soil 2, respectively) was observed during repeated phytoextraction (Table S7). The lower soil pH may have promoted the dissolution of Fe/Mn oxides and release of fixed Zn, thus rebalancing the Fe/Mn oxide-bound Zn fraction with the exchangeable Zn pool, and thereby increasing the exchangeable Zn concentration by 1.3–9.1 folds.

The metal isotope ratios of bulk soils before the first, third and sixth seasons were calculated from the metal mass balance of all aggregate size fractions (Table S8) and used to study isotopic variations during repeated phytoextraction. During the five successive seasons, the Zn isotope composition of the two bulk soils remained stable ($\Delta^{66}Zn_{C6-C1} = 0.04 \pm 0.04$‰ for Soil 1 and 0.03 ± 0.04‰ for Soil 2). Additionally, there was no detectable variation within analytical uncertainty in the Zn isotope compositions of the four aggregate size fractions during the long-term phytoextraction ($\Delta^{66}Zn_{C6-C1} = -0.01 \pm 0.06$‰ to 0.07 ± 0.06‰, Table 2). A low isotope fractionation factor for plant uptake of Zn in combination with the relatively low extent of Zn loss induced by plant uptake may be responsible for the negligible Zn isotope fractionation in soils. However, even for the 5–50 and 1–5 μm size fractions with substantial declines in Zn concentrations (decreases of 16–34%), the $\delta^{66}Zn$ values remained essentially stable over the six phytoextraction seasons. Once Zn in the soil solution was depleted by plant roots, Zn bound to the soil solid phase would be released for continuous plant uptake, driven by equilibrium partitioning. Therefore, isotope fractionation might occur during Zn release from solid phases to soil solution as a consequence of solid-liquid partitioning. The Tessier extraction results show that the decrease in Fe/Mn oxide bound Zn predominantly accounted for the Zn concentration decrease in the 5–50 and 1–5 μm size fractions during repeated phytoextraction. This suggests that the Zn released from Fe/Mn oxides dominated the Zn taken up by *S. plumbizincicola*. In the studies of Zn adsorption to Mn oxides such as todorokite (Wang et al., 2022) and birnessite (Wang et al., 2023), negligible Zn isotope fractionation was observed between the dissolved Zn and Zn retained on the solid minerals ($\Delta^{66}Zn_{solid\text{-}solution} = -0.10$ to 0.05‰) at pH 6–8. The soil pH of the 5–50 and 1–5 μm size fractions from both soils studied here were within this range (Table S9) and thus only limited or no Zn isotope fractionation is expected for the release of Zn bound to Mn oxides. These findings can hence account for the small $\Delta^{66}Zn_{C6-C1}$ values that were observed for the 5–50 and 1–5 μm size fractions.

Considering dynamic changes of the $\delta^{66}Zn$ values for the plant shoots during repeated phytoextraction, there were no significant changes from the first to the third season but the shoots became marginally heavier (by 0.08‰) from the third to the sixth season (Fig. 4a). As *S. plumbizincicola* allocates >95% of Zn and Cd taken up by roots to its aerial parts, the metal isotope composition of the shoots effectively represents those of the whole plant (Zhou et al., 2023). In the first two seasons, only a small fraction of the bulk soil Zn (2–3%, Table 1) was removed by the plants. As a consequence, the Zn isotope composition of the bulk soils and the available Zn pools in soils remained almost unchanged, and the $\delta^{66}Zn$ values of the shoots were also essentially constant.

From the third to sixth season, Zn in the shoots gradually became isotopically heavier ($\Delta^{66}Zn_{C6-C3} = 0.08 \pm 0.04$‰ for Soil 1 and 0.08 ± 0.03‰ for Soil 2) may reflect processes that impacted the $\delta^{66}Zn$ of the bioavailable Zn pool and/or isotope fractionation during plant uptake. The results imply that the bioavailable Zn pool accessed by the plant roots became isotopically heavier as phytoextraction proceeded. If sufficient Zn is available, plants tend to preferentially take up light Zn isotopes from the growth media (Wiggenhauser et al., 2022), leading to an enrichment of heavy Zn isotopes in the remaining bioavailable pool. In addition, Houben et al. (2014) found that root-induced soil acidification released heavier Zn isotopes from the soil to soil leachates compared to soil controls with no plants present. Consistent with this, soil acidification during repeated phytoextraction in the current study may have

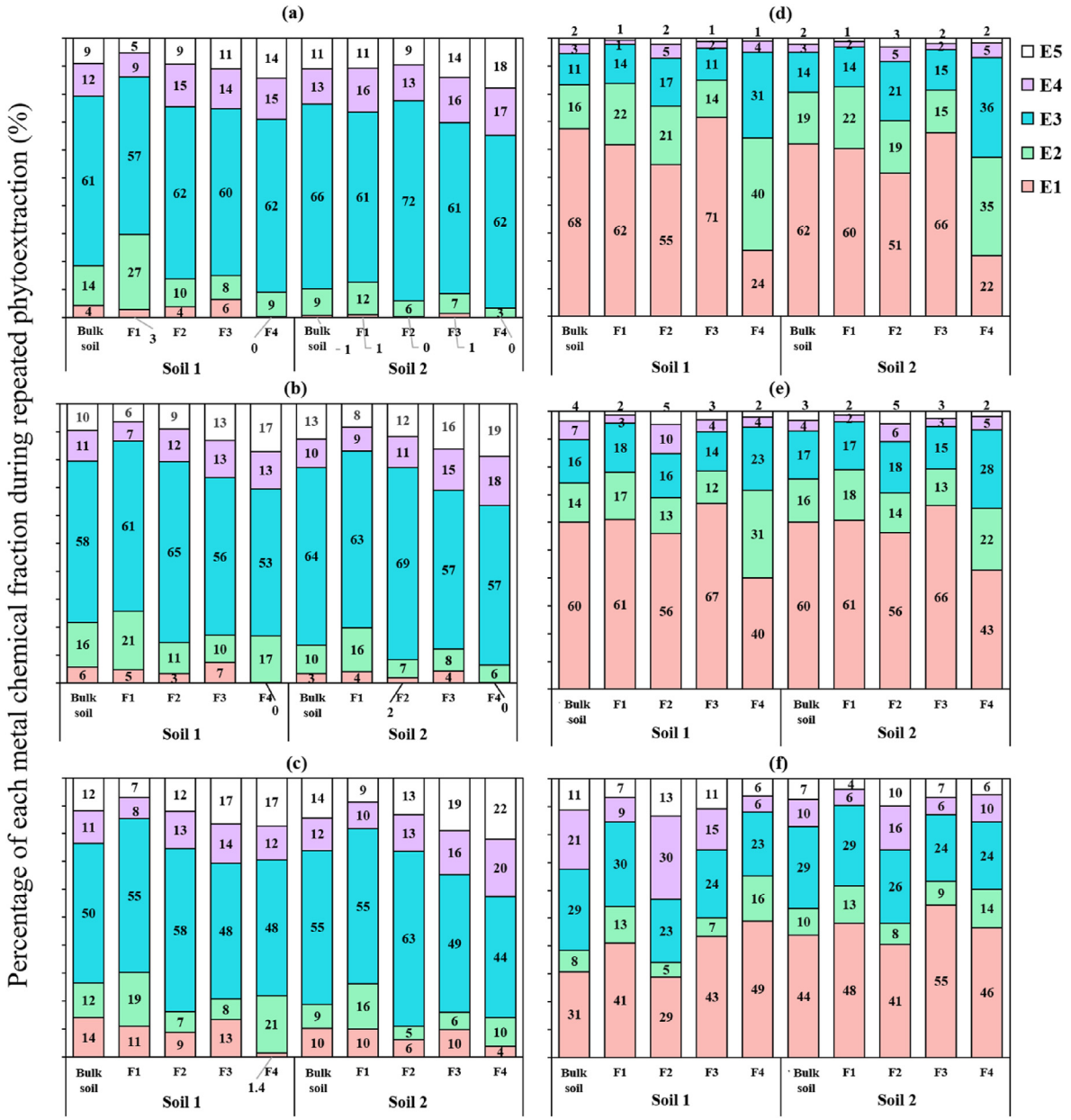


Fig. 2. Fractions (in %) of total Zn (a) before the first season, (b) before the third season, (c) before the sixth season; and of total Cd (d) before the first season, (e) before the third season, and (f) before the sixth season in different chemical fractions for the aggregates of both soils. Soil aggregate size fractions: F1, 50–250 μm; F2, 5–50 μm; F3, 1–5 μm; F4, <1 μm. Chemical fractions: E1, exchangeable metal; E2, metal bound to carbonates; E3, metal bound to iron and manganese oxides, E4, metal bound to organic matter; E5, residual metal. Data for samples from before phytoextraction are from our previous study (Zhou et al., 2024).

induced the release of isotopically heavier Zn from the soil solids for plant uptake.

3.3. Cadmium changes in the plant-soil system during repeated phytoextraction

During the five consecutive seasons, the total Cd concentrations of Soils 1 and 2 decreased by 89% and 78%, respectively (Table 1). Comparing the total Cd concentrations for the four aggregate size fractions during remediation, similar fractional decreases were observed after the fifth season for Soil 1 (by 87–92%) and Soil 2 (by 72–80%) (Table 1). However, the first two seasons of the phytoextraction led to more pronounced decreases in Cd concentrations for the 5–50, 1–5 and <1 μm size fractions than for the 50–250 μm size fraction. This indicates that Cd in the three finer size fractions was more readily available to the plants than that in the 50–250 μm aggregates during the early period of long-term phytoextraction.

Chemical fractionation analysis shows that Cd in the 50–250, 5–50 and 1–5 μm size fractions before phytoextraction was present mainly in the exchangeable fraction (62% of total Cd) (Fig. 2d). After successive phytoextraction over five seasons, the exchangeable Cd showed the largest decrease in absolute concentration in these three aggregate size fractions, and this contributed, on average, 62% to the total decline of the bulk soil Cd concentration (Table S6). Based on the concentration decreases observed for the five chemical fractions during phytoextraction, the exchangeable and carbonate-bound Cd were the two most bioavailable forms in the 1–250 μm size fractions (Fig. 2d–f). However, relative to the 1–250 μm aggregates of, the <1 μm aggregates with higher pH and higher contents of Fe and Mn oxides before phytoextraction (Table S9), initially hosted a lower fraction of exchangeable Cd but larger fractions of

Table 2
Cd and Zn isotope compositions of aggregate of different size fractions during repeated phytoextraction.

Soil	Aggregate size fraction	δ^{66}Zn (‰)			$\delta^{114/110}$Cd (‰)		
		C1	C3	C6	C1	C3	C6
Soil 1	Bulk soil	0.22 ± 0.03 b	0.30 ± 0.03 a	0.23 ± 0.01 b	−0.13 ± 0.01 a	−0.08 ± 0.04 a	−0.27 ± 0.04 b
	F1	0.29 ± 0.04	0.32 ± 0.03	0.33 ± 0.04	−0.09 ± 0.02	−0.14 ± 0.02	−0.20 ± 0.03
	F2	0.26 ± 0.04	0.24 ± 0.05	0.28 ± 0.04	−0.12 ± 0.02	−0.13 ± 0.02	−0.23 ± 0.03
	F3	0.22 ± 0.05	0.28 ± 0.04	0.28 ± 0.06	−0.05 ± 0.03	−0.12 ± 0.02	−0.19 ± 0.03
	F4	0.28 ± 0.04	0.33 ± 0.03	0.30 ± 0.03	−0.02 ± 0.03	−0.06 ± 0.03	−0.14 ± 0.07
Soil 2	Bulk soil	0.22 ± 0.02 a	0.29 ± 0.05 a	0.25 ± 0.02 a	−0.06 ± 0.02 b	0.00 ± 0.02 a	−0.18 ± 0.02 c
	F1	0.28 ± 0.04	0.29 ± 0.04	0.30 ± 0.05	−0.02 ± 0.03	−0.04 ± 0.03	−0.07 ± 0.03
	F2	0.22 ± 0.05	0.23 ± 0.04	0.21 ± 0.04	−0.06 ± 0.02	−0.07 ± 0.03	−0.10 ± 0.02
	F3	0.20 ± 0.05	0.26 ± 0.04	0.27 ± 0.04	−0.02 ± 0.02	−0.05 ± 0.03	−0.13 ± 0.07
	F4	0.28 ± 0.04	0.27 ± 0.05	0.29 ± 0.04	0.01 ± 0.02	−0.01 ± 0.03	−0.01 ± 0.03

The errors shown for the mean $\delta^{114/110}$Cd values are ± 2SE, (i) for the bulk soils, based on analyses of three replicate samples; (ii) for the aggregate size fractions where only one sample was analyses, based on the within-run (internal) error of the sample run. Cadmium and Zn isotope compositions of bulk soils before phytoextraction and after the fifth season were measured at the University of Science and Technology of China (Zhou et al., 2020) whereas the other data were obtained at Imperial College London, UK. Different lowercase letters indicate significant differences in the bulk soil metal isotopic values for different phytoextraction periods at $p < 0.05$. C1, C3 and C6, before the first, third and sixth season. Soil aggregate size fractions: F1, 50–250 μm; F2, 5–50 μm; F3, 1–5 μm; F4, < 1 μm.

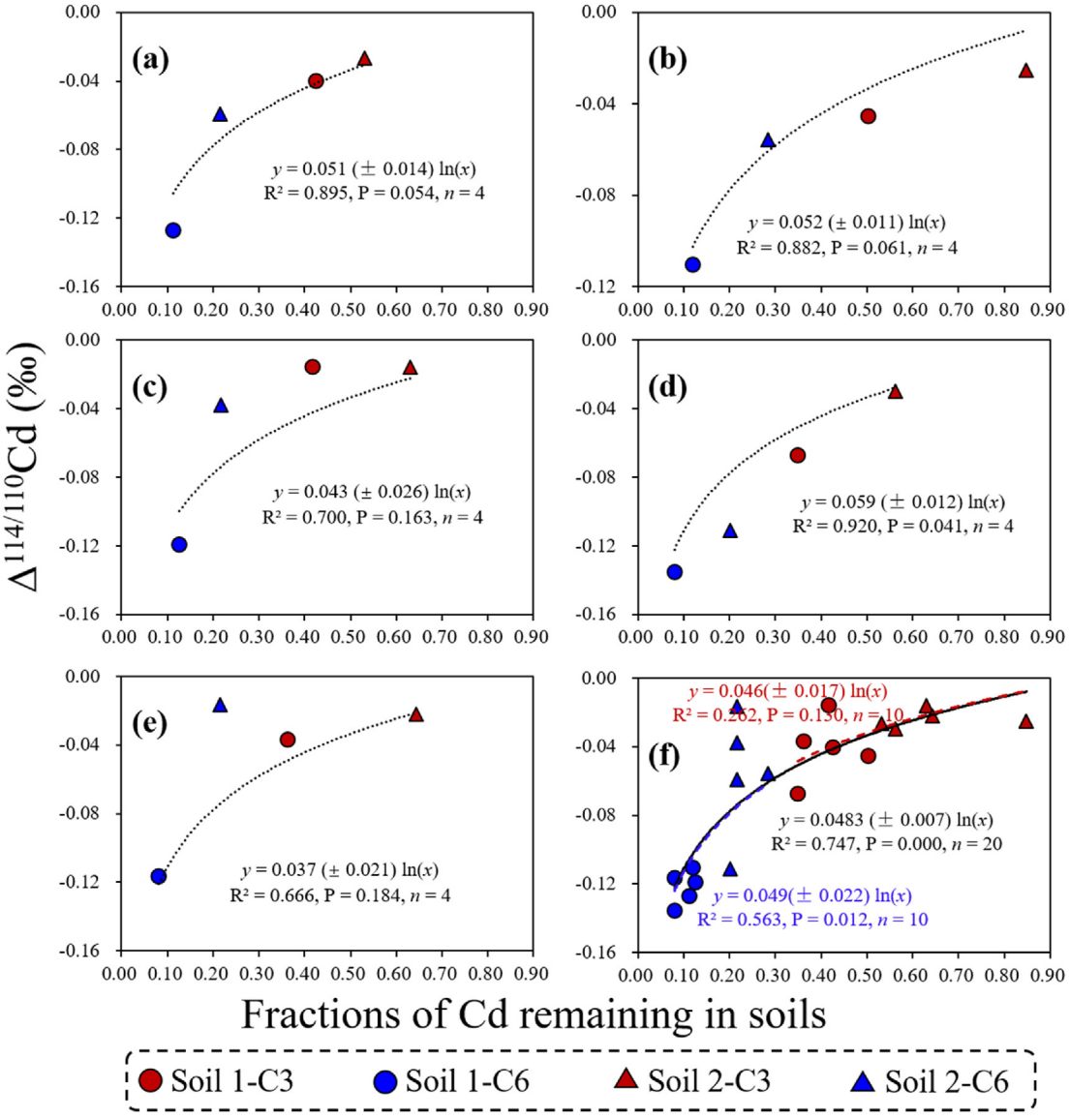


Fig. 3. Plots of apparent Cd isotope fractionation ($\Delta^{114/110}$Cd) between bulk soils or soil aggregate size fractions after phytoextraction and the initial soils and soil aggregate size fractions. The individual panels show the results for (a) bulk soils, the aggregate size fractions (b) 50–250 μm, (c) 5–50 μm, (d) 1–5 μm, and (e) < 1 μm. Panel (f) combines the results for all aggregate size fractions during repeated phytoextraction (the black dotted line for all samples, the red solid line for samples of the first two cropping cycles and the blue solid line for samples of the late three cropping cycles). The value in brackets after the slope denotes the confidence interval at $p < 0.05$.

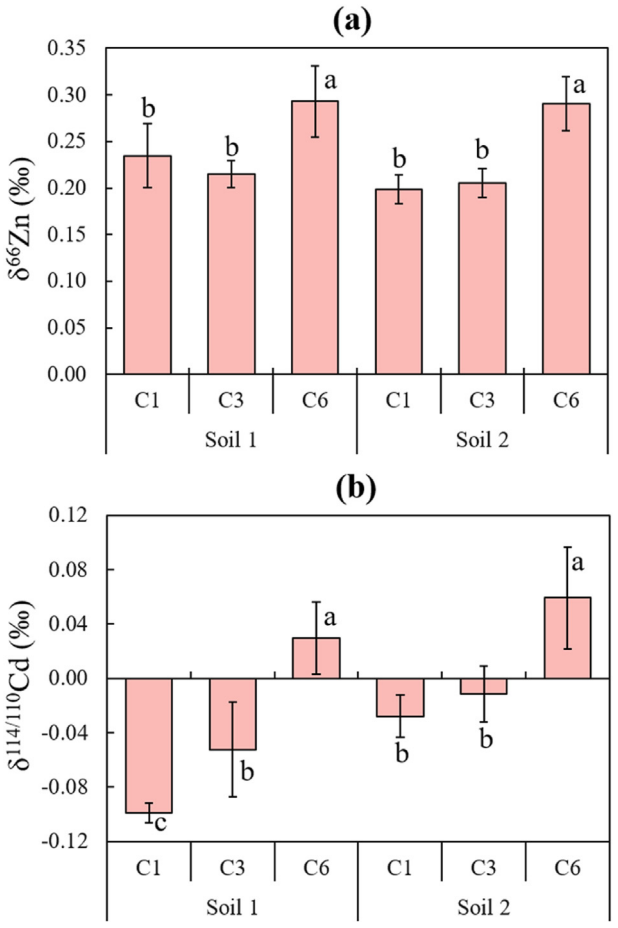


Fig. 4. Isotope compositions of (a) Zn and (b) Cd in shoots during repeated phytoextraction. Data are expressed as mean ± 2SE, based on analyses of three replicate samples. The isotope data for shoots from the first season were measured at the University of Science and Technology of China (Zhou et al., 2020) whereas the other data were obtained at Imperial College London, UK. Different lowercase letters indicate significant differences in the isotope compositions of the shoots at different phytoextraction periods at $p < 0.05$. C1, in the first season; C3, in the third season; C6, in the sixth season.

carbonate- and Fe/Mn oxide-bound Cd (Fig. 2). After the fifth season, the exchangeable Cd fraction in the <1 μm aggregates almost doubled but the fractions of carbonate- and Fe/Mn oxide-bound Cd decreased markedly. The largest absolute decline in the carbonate-bound Cd concentration contributes about 40% to the decline in the total Cd concentrations observed for the <1 μm size fraction. These results indicate that the carbonate- and Fe/Mn oxide-bound Cd is more accessible to plants from the <1 μm aggregates rather than from the coarser aggregates.

The <1 μm aggregates had the smallest fractions of exchangeable Cd and should hence offer less bioavailable Cd. However, all four aggregate size fractions exhibited similar decreases in Cd concentration during the five cropping cycles. Similar results were reported by Li et al. (2014a,b) who found that plant metal uptake was enhanced for finer aggregates. Metals in smaller aggregates can be more accessible to plant roots due to the high aggregate specific surface area, which provides greater root-aggregate contact (Chen et al., 2008). Considering the exchangeable and carbonate-bound Cd as the fractions that are bioavailable to plants, the total Cd mass in the bioavailable pool was able to balance the total Cd uptake by the plants in the first two seasons. Therefore, during the early period of remediation, the hyperaccumulator took up the readily Cd fractions from the soils. However, in the last three seasons, the decrease in the amount of bioavailable Cd in the bulk soils (8.97 and 11.7 mg in Soil 1 and Soil 2, respectively) could not account for the total amount of Cd removed by *S. plumbizincicola* (10.5 and 11.9 mg in Soil 1 and Soil 2, respectively), particularly in Soil 1. This indicates the mobilization of Cd from potentially available pools (e.g., Fe/Mn oxide-bound Cd). Cadmium hyperaccumulators such as *S. alfredii* (a species closely related to *S. plumbizincicola* in the family *Crassulaceae*) were reported to exudate organic acids to dissolve carbonate- and Fe/Mn oxide-bound Cd (Li et al., 2013; Tao et al., 2016). In our experiments, *S. plumbizincicola* may have adopted similar mechanisms to *S. alfredii* to access extra Cd from soil aggregates, as suggested by the decreasing soil pH value during repeated phytoextraction (Table S7).

After repeated phytoextraction, the bulk soil isotope composition was significantly lighter for Soil 1 (by −0.13 ± 0.02‰) and slightly lighter for Soil 2 (by −0.06 ± 0.03‰) (Table S8). This suggests that the heavy Cd isotopes of soils were preferentially depleted by *S. plumbizincicola*. Fitting of a Rayleigh model to the data for both soils yielded a fractionation factor ε_{Cd} of 0.05 ± 0.01‰, which characterizes the overall Cd isotope fractionation that generated by plant Cd uptake from soils (Fig. 3a). The four aggregate size fractions showed either lighter or unchanged Cd isotope composition after the fifth season with $\Delta^{114/110}Cd_{C6\text{-}C1}$ values (which denote the differences in the $\delta^{114/110}Cd$ values of soil aggregates between the first and sixth season) from −0.14 ± 0.04 to −0.02 ± 0.04‰. The phytoextraction thereby led to a more pronounced enrichment of light Cd isotopes in the aggregate size fractions of Soil 1 ($\Delta^{114/110}Cd_{C6\text{-}C1}$ = −0.14 to −0.11‰) than those of Soil 2 ($\Delta^{114/110}Cd_{C6\text{-}C1}$ = −0.08 to −0.02‰). In addition, the depletion of heavy Cd isotopes in the aggregates of Soil 1 for the last three seasons ($\Delta^{114/110}Cd_{C6\text{-}C3}$ = −0.10 to −0.06‰ with a mean of −0.08‰) was more pronounced compared to that observed for the first two seasons ($\Delta^{114/110}Cd_{C3\text{-}C1}$ = −0.07 to −0.01‰ with a mean of −0.04‰) (Table 2). Soil 1 is an acidic soil with high Cd bioavailability and the Cd removal efficiency for the first two seasons reached 57.4% (Table 1). Cadmium release due to root exudation of organic acids was likely enhanced during the last three seasons and this would have further enhanced the depletion of heavy Cd isotopes in the soil aggregates.

The isotope data for the aggregate size fractions (particularly for the 50–250 and 1–5 μm size fractions) are also in good accord with Rayleigh fractionation curves and they yielded fractionation factors ε_{Cd} that are essentially identical to one another and the bulk value at $\varepsilon_{Cd} \approx$ 0.04–0.06‰ (Fig. 3b–e). This suggests that similar mechanisms controlled the overall Cd release from the different aggregate size fractions to plants.

The shoots showed a gradually increasing trend in $\delta^{114/110}Cd$ after the first season, with $\Delta^{114/110}Cd_{C6\text{-}C1}$ = 0.13 ± 0.03‰ for Soil 1 and 0.09 ± 0.04‰ for Soil 2 (Fig. 4b). This trend toward the gradual heavier Cd isotope composition in plants was further supported by the mass balance calculation of Cd isotopes in the bulk soils during repeated phytoextraction (Section S3 of the Supplementary Materials). As shown in Table S10, the calculated isotope composition of Cd taken up by plant in the last three seasons was clearly heavier than that in the first two seasons in both soils ($\Delta^{114/110}Cd$ = 0.14‰ in Soil 1 and 0.24‰ in Soil 2, respectively). During repeated phytoextraction, the bulk soil Cd generally became isotopically lighter, whilst Cd in the plant shoots was isotopically heavier. Consequently, the apparent Cd isotope fractionation between plants and soils ($\Delta^{114/110}Cd_{shoot\text{-}soil}$) increased significantly from −0.02–0.00‰ for the first season to 0.15–0.24‰ for the sixth season (Fig. S2). This is indicative of processes in the soil-plant system which enriched heavy Cd isotopes in plants. Root mobilization (e.g., via exudation of organic acids) and high-affinity transport are reported to favor the uptake of heavy Cd isotopes. For example, complexation of Cd with oxygen-containing organic ligands favors heavy Cd isotopes based on the predictions of density functional theory (Zhao et al., 2021). High-affinity transporters are highly synthetized and function predominantly for metal uptake at low supply levels (Riaz et al., 2021; Zhou et al., 2023), leading to the enrichment of heavier isotopes. This is further supported by the observation that *S. plumbizincicola* supplied with 1 μM Cd exhibits a stronger enrichment of heavy Cd isotopes during uptake

than plants supplied with 50 μM Cd ($\delta^{114/110}$Cd = 0.02‰ at 1 μM Cd and −0.26‰ at 50 μM Cd, respectively; Zhou et al., 2023).

The combined analyses of Cd concentration, chemical fraction and isotope composition consistently imply the occurrence of Cd mobilization in the soils and soil aggregates, particularly at the later stages of the long-term phytoextraction. As to what triggered the root exudation of organic acids to dissolve Cd, there are two possible explanations. Firstly, Cd hyperaccumulators show a very strong ability to continuously take up metals from soils, to the extent that it could be suggested that Cd may even play some physiological roles in these species. Cadmium addition (100 μM) to the nutrient solution increased the biomass of root, stem and leaf for the Cd hyperaccumulator *S. alfredii* relative to the control (Li et al., 2009). Also, increasing Cd concentration in the hydroponic solution increased the carbonic anhydrase activities of the hyperaccumulators *N. caerulescens* (Liu et al., 2008) and *P. divaricata* Vant (Liu et al., 2016). It is very likely that the hyperaccumulators adopt active mechanisms such as root secretion of organic acids to access additional Cd pools under low Cd supplies. Another explanation is that nutrient deficiency triggered root exudation and promoted soil Cd dissolution. We measured the available calcium (Ca), magnesium (Mg), Fe and Mn concentrations during repeated phytoextraction (Table S11). Soil available Ca and Mg showed a general decreasing trend as the experiment proceeded. Plants from the Crassulaceae family (*S. plumbizincicola* is a member of this family) have strong demand for Ca to act as the counter cations to large amounts carboxylates in vacuoles (Sun et al., 2019). It is also likely that the decreasing Ca or Mg concentration in soil available pool triggered the enhanced root exudation. Further studies are required to verify the correct explanation for Cd mobilization.

The plant uptake strategy governs the isotope fractionation factor incurred during Cd uptake by plants from soils. To investigate whether there is a change in Cd uptake strategy during the long-term phytoextraction, Rayleigh fitting was performed for different phytoextraction periods and this yielded isotope fractionation factors of 0.046 ± 0.017‰ and 0.049 ± 0.022‰ for the first two and the last three seasons, respectively (Fig. 3f). The similarity of these fractionation factors suggests that *S. plumbizincicola* maintained a similar strategy to take up Cd throughout the phytoextraction period. In addition, the plants progressed to heavier Cd isotope compositions as phytoextraction continued, in keeping with the depletion of heavy Cd isotopes in the bulk soils after six cropping cycles (Table 2 and Fig. 4). Taken together, this indicates that the continuing enrichment of isotopically heavier Cd in the plants during long-term phytoextraction are achieved by gradually increasing contributions of root mobilization and/or high-affinity uptake and do not involve any clear switch in the Cd uptake strategy of *S. plumbizincicola*.

3.4. Implications and perspectives

Here stable isotope analysis reveals different isotopic behaviors of Zn and Cd from soil aggregates to plants (Zn, no significant isotope fractionation; Cd, similar isotope fractionation in the four aggregate size fractions). This observed difference could be ascribed to the different abilities of *S. plumbizincicola* to hyperaccumulate the two metals and their distinct supply levels in soils. The Zn bioconcentration factor (8.31 ± 0.74) in *S. plumbizincicola* is much lower than that of Cd (41.2 ± 3.47) (Wu et al., 2018; Zhou et al., 2019) while the Zn concentrations of the studied soils were two orders of magnitude higher than those of Cd. In addition, in the later stages of the phytoextraction experiment, ~80% of the Cd originally present in the bulk soils had been removed by the plants, leaving behind a remaining soil Cd fraction with lower bioavailability. In contrast to Cd, only about 20% of soil Zn was removed by the plants. Therefore, even in the last stages of the repeated phytoextraction, *S. plumbizincicola* could readily access sufficient Zn from the available pool and preferentially take up Zn from the aggregates with higher Zn availability. In contrast, Cd supply in the soils was much more limited and *S. plumbizincicola* hence accessed Cd from all aggregate size fractions with low selectivity.

The particle or aggregate size of solids can markedly impact the biogeochemical processes of metals (Bianchi et al., 2018) and consequently alter their isotope fractionations. Further studies are worthwhile on the isotope fractionation affected by soil aggregate size in soils with varied physiochemical properties because soil properties are the crucial factors controlling metal partition in soil aggregate. In addition, Cd isotopes behaved similarly in soil aggregates of different size fractions during repeated phytoextraction due to the limited Cd supply in soil. Cadmium supply condition in the growth medium plays an important role in influencing Cd isotope fractionation in the soil-plant system and different cadmium isotope fractionations can be expected in soil aggregates of different size fractions during repeated phytoextraction if soils with contrasting Cd pollution levels are used. However, in the present study, even long-term phytoextraction was associated with negligible Zn isotope fractionation between plants and soil aggregate of different size fractions. The data suggest that isotope variation of total Zn in soil may not be a sensitive or effective indicator in response to plant activities during phytoextraction. Instead, Zn isotope composition of the plant-available pool in the soil aggregates of different sizes is expected to be greatly altered by plant uptake. Therefore, it will be of interest to determine possible metal isotope fractionations in the accessible Zn pools of different aggregate size fractions during repeated phytoextraction. Such analysis would provide further constraints on the importance of aggregate size effects on the metal isotope fractionations that are associated with phytoremediation practices.

CRediT authorship contribution statement

Jiawen Zhou: Writing – review & editing, Writing – original draft, Formal analysis, Data curation, Conceptualization. **Jingqi Dong:** Writing – review & editing. **Rebekah E.T. Moore:** Writing – review & editing, Writing – original draft, Formal analysis. **Mark Rehkämper:** Writing – review & editing, Supervision, Methodology. **Katharina Kreissig:** Methodology. **Barry Coles:** Methodology. **Ting Gao:** Writing – original draft, Formal analysis. **Peter Christie:** Writing – review & editing. **Longhua Wu:** Writing – review & editing, Validation, Supervision, Funding acquisition, Conceptualization.

Declaration of competing interest

The authors declare that they have no known competing financial interests or personal relationships that could have appeared to influence the work reported in this paper.

Acknowledgments

This study was supported by the National Natural Science Foundation of China (No. 42107033 and 42377022), the Natural Science Foundation of Jiangsu Province, China (No. BK20210996), China Postdoctoral Science Foundation (No. 2022M713235) and a Royal Society International Exchange grant (IEC\NSFC\211075).

Appendix A. Supplementary data

Supplementary data to this article can be found online at https://doi.org/10.1016/j.seh.2025.100129.

References

Abouchami, W., Galer, S.J.G., Horner, T.J., Rehkämper, M., Wombacher, F., Xue, Z.C., Lambelet, M., Gault-Ringold, M., Stirling, C.H., Schönbächler, M., Shiel, A.E., Weiss, D., Holdship, P.F., 2013. A common reference material for cadmium isotope studies - NIST SRM 3108. Geostand. Geoanal. Res. 37 (1), 5–17. https://doi.org/10.1111/j.1751-908X.2012.00175.x.

Archer, C., Andersen, M.B., Cloquet, C., Conway, T.M., Dong, S., Ellwood, M., Moore, R., Nelson, J., Rehkämper, M., Rouxel, O., Samanta, M., Shin, K.-C., Sohrin, Y., Takano, S., Wasylenki, L., 2017. Inter-calibration of a proposed new primary

reference standard AA-ETH Zn for zinc isotopic analysis. J. Anal. At. Spectrom. 226, 280–297. https://doi.org/10.1039/c6ja00282j.
Bacq-Labreuil, A., Crawford, J., Mooney, S.J., Neal, A.L., Ritz, K., 2019. Cover crop species have contrasting influence upon soil structural genesis and microbial community phenotype. Sci. Rep. 9, 7473. https://doi.org/10.1038/s41598-019-43937-6.
Banerjee, U.S., Guo, Z.H., Zhou, K.G., Chai, L.Y., 2017. Distribution and plant availability of Cd, Pb, Cu and As in different particle size soil fractions. J. Indian Chem. Soc. 94 (9), 1029–1035.
Barati, E., Moore, R.E.T., Ullah, I., Kreissig, K., Coles, B.J., Dunwell, J.M., Rehkämper, M., 2023. An investigation of zinc isotope fractionation in cacao (*Theobroma cacao* L.) and comparison of zinc and cadmium isotope compositions in hydroponic plant systems under high cadmium stress. Sci. Rep. 13, 4682. https://doi.org/10.1038/s41598-023-30899-z.
Bianchi, D., Weber, T.S., Kiko, R., Deutsch, C., 2018. Global niche of marine anaerobic metabolisms expanded by particle microenvironments. Nat. Geosci. 11, 263–268. https://doi.org/10.1038/s41561-018-0081-0.
Chen, W.P., Chany, A.C., Wu, L.S., Zhang, Y.S., 2008. Metal uptake by corn grown on media treated with particle-size fractionated biosolids. Sci. Total Environ. 392, 166–173. https://doi.org/10.1016/j.scitotenv.2007.11.019.
Dabkowska-Naskret, H., 2003. The role of organic matter in association with zinc in selected arable soils from Kujawy Region, Poland. Org. Geochem. 34, 645–649. https://doi.org/10.1016/S0146-6380(03)00019-6.
Gruter, R., Costerousse, B., Mayer, J., Mader, P., Thonar, C., Frossard, E., Schulin, R., Tandy, S., 2019. Long-term organic matter application reduces cadmium but not zinc concentrations in wheat. Sci. Total Environ. 669, 608–620. https://doi.org/10.1016/j.scitotenv.2019.03.112.
Houben, D., Sonnet, P., Tricot, G., Mattielli, N., Couder, E., Opfergelt, S., 2014. Impact of root-induced mobilization of zinc on stable Zn isotope variation in the soil-plant system. Environ. Sci. Technol. 48, 7866–7873. https://doi.org/10.1021/es5002874.
Huang, B., Yuan, Z.J., Li, D.Q., Zheng, M.G., Nie, X.D., Liao, Y.S., 2020. Effects of soil particle size on the adsorption, distribution and migration behaviors of heavy metal(loid)s in soil: a review. Environ. Sci.: Process. Impacts 22, 1596–1615. https://doi.org/10.1039/d0em00189a.
Huynh, T.T., Zhang, H., Laidlaw, W.S., Singh, B., Baker, A.J.M., 2010. Plant-induced changes in the bioavailability of heavy metals in soil and biosolids assessed by DGT measurements. J. Soils Sediments 10, 1131–1141. https://doi.org/10.1007/s11368-010-0228-0.
Koopmans, G.F., Romkens, P.F.A.M., Fokkema, M.J., Song, J., Luo, Y.M., Japenga, J., Zhao, F.J., 2008. Feasibility of phytoextraction to remediate cadmium and zinc contaminated soils. Environ. Pollut. 156, 905–914. https://doi.org/10.1016/j.envpol.2008.05.029.
Lamb, D.T., Kader, M., Ming, H., Wang, L., Abbasi, S., Megharaj, M., Naidu, R., 2016. Predicting plant uptake of cadmium: validated with long-term contaminated soils. Ecotoxicology 25, 1563–1574. https://doi.org/10.1007/s10646-016-1712-0.
Li, G., Tong, F.P., Liu, Z.H., 2012. Analysis on pollution of heavy metal in Shuikoushan Pb-Zn mining and smelting area in Hengyang. J. Centr. South Univer. Forestry & Tech. 32 (7), 105–109. https://doi.org/10.14067/j.cnki.1673-923x.2012.07.007 (in Chinese).
Li, M.Y., Ren, L.H., Zhang, J.C., Luo, L., Qin, P.F., Zhou, Y.Y., Huang, C., Tang, J.Y., Huang, H.L., Chen, A.W., 2019. Population characteristics and influential factors of nitrogen cycling functional genes in heavy metal contaminated soil remediated by biochar and compost. Sci. Total Environ. 651, 2166–2174. https://doi.org/10.1016/j.scitotenv.2018.10.152.
Li, T.Q., Liang, C.F., Han, X., Yang, X.E., 2013. Mobilization of cadmium by dissolved organic matter in the rhizosphere of hyperaccumulator *Sedum alfredii*. Chemosphere 91, 970–976. https://doi.org/10.1016/j.chemosphere.2013.01.100.
Li, T.Q., Yang, X.E., Lu, L.L., Islam, E., He, Z.L., 2009. Effects of zinc and cadmium interactions on root morphology and metal translocation in a hyperaccumulating species under hydroponic conditions. J. Hazard Mater. 169 (1–3), 734–741. https://doi.org/10.1016/j.jhazmat.2009.04.004.
Li, X.P., Gao, Y., Zhang, M., Zhang, Y., Zhou, M., Peng, L.Y., He, A., Zhang, X., Yan, X.Y., Wang, Y.H., Yu, H.T., 2020. In vitro lung and gastrointestinal bioaccessibility of potentially toxic metals in Pb-contaminated alkaline urban soil: the role of particle size fractions. Ecotoxicol. Environ. Saf. 190, 110151. https://doi.org/10.1016/j.ecoenv.2019.110151.
Li, Z., Jia, M.Y., Wu, L.H., Christie, P., Luo, Y.M., 2016. Changes in metal availability, desorption kinetics and speciation in contaminated soils during repeated phytoextraction with the Zn/Cd hyperaccumulator *Sedum plumbizincicola*. Environ. Pollut. 209, 123–131. https://doi.org/10.1016/j.envpol.2015.11.015.
Li, Z., Wu, L.H., Hu, P.J., Luo, Y.M., Zhang, H., Christie, P., 2014a. Repeated phytoextraction of four metal-contaminated soils using the cadmium/zinc hyperaccumulator *Sedum plumbizincicola*. Environ. Pollut. 189, 176–183. https://doi.org/10.1016/j.envpol.2014.02.034.
Li, Z., Wu, L.H., Luo, Y.M., Christie, P., 2014b. Dynamics of plant metal uptake and metal changes in whole soil and soil particle fractions during repeated phytoextraction. Plant Soil 374, 857–869. https://doi.org/10.1007/s11104-013-1927-2.
Liu, L., Wu, L.H., Luo, Y.M., Zhang, C.B., Jiang, Y.G., Qiu, X.Y., 2010. The impact of a copper smelter on adjacent soil zinc and cadmium fractions and soil organic carbon. J. Soils Sediments 10, 808–817. https://doi.org/10.1007/s11368-010-0227-1.
Liu, M.Q., Yanai, J.T., Jiang, R.F., Zhang, F.S., McGrath, S.P., Zhao, F.J., 2008. Does cadmium play a physiological role in the hyperaccumulator *Thlaspi caerulescens*? Chemosphere 71 (7), 1270–1283. https://doi.org/10.1016/j.chemosphere.2007.11.063.
Liu, S.H., Tang, Y.T., Qiu, R.L., Ge, R.G., Ji, X.H., 2016. Responses of carbonic anhydrase to cadmium in the zinc/cadmium hyperaccumulator *Picris divaricata* Vant. Pedosphere 26 (5), 709–716. https://doi.org/10.1016/S1002-0160(15)60081-9.
Liu, M.S., Zhang, Q., Zhang, Y.N., Zhang, Z.F., Huang, F., Yu, H.M., 2020. High-precision Cd isotope measurements of soil and rock reference materials by MC-ICP-MS with double spike correction. Geostand. Geoanal. Res. 44 (1), 169–182. https://doi.org/10.1111/ggr.12291.
Luo, X.S., Yu, S., Li, X.D., 2011. Distribution, availability, and sources of trace metals in different particle size fractions of urban soils in Hong Kong: implications for assessing the risk to human health. Environ. Pollut. 159, 1317–1326. https://doi.org/10.1016/j.envpol.2011.01.013.
Moore, R.E.T., Larner, F., Coles, B.J., Rehkämper, M., 2017. High precision zinc stable isotope measurement of certified biological reference materials using the double spike technique and multiple collector-ICP-MS. Anal. Bioanal. Chem. 409 (11), 2941–2950. https://doi.org/10.1007/s00216-017-0240-y.
Moore, R.E.T., Ullah, I., de Oliveira, V.H., Hammond, S.J., Strekopytov, S., Tibbett, M., Dunwell, J.M., Rehkämper, M., 2020. Cadmium isotope fractionation reveals genetic variation in Cd uptake and translocation by *Theobroma cacao* and role of natural resistance-associated macrophage protein 5 and heavy metal ATPase-family transporters. Horticulture Res. 7 (1), 71. https://doi.org/10.1038/s41438-020-0292-6.
Quenea, K., Lamy, I., Winterton, P., Bermond, A., Dumat, C., 2009. Interactions between metals and soil organic matter in various particle size fractions of soil contaminated with waste water. Geoderma 149, 217–223. https://doi.org/10.1016/j.geoderma.2008.11.037.
Riaz, U., Aslam, A., Zaman, Q.U., Javeid, S., Gul, R., Iqbal, S., Javid, S., Murtaza, G., Jamil, M., 2021. Cadmium contamination, bioavailability, uptake mechanism and remediation strategies in soil-plant-environment system: a critical review. Curr. Anal. Chem. 17 (1), 49–60. https://doi.org/10.2174/1573411016999200817174311.
Sheoran, V., Sheoran, A.S., Poonia, P., 2016. Factors affecting phytoextraction: a review. Pedosphere 26 (2), 148–166. https://doi.org/10.1016/S1002-0160(15)60032-7.
Shi, J.D., Zhao, D., Ren, F.T., Huang, L., 2023. Spatiotemporal variation of soil heavy metals in China: the pollution status and risk assessment. Sci. Total Environ. 871, 161768. https://doi.org/10.1016/j.scitotenv.2023.161768.
Sun, X., Wu, L.H., Christie, P., Luo, Y.M., Fornara, D.A., 2019. Root-induced soil acidification and cadmium mobilization in the rhizosphere of *Sedum plumbizincicola*: evidence from a high-resolution imaging study. Plant Soil 436, 267–282. https://doi.org/10.1007/s11104-018-03930-w.
Suo, Y.G., Tang, N., Li, H., Corti, G., Jiang, L.J., Huang, Z.L., Zhang, Z.G., Huang, J., Wu, Z.J., Feng, C.L., Zhang, X., 2021. Long-term effects of phytoextraction by a poplar clone on the concentration, fractionation, and transportation of heavy metals in mine tailings. Environ. Sci. Pollut. Control Ser. 28, 47528–47539. https://doi.org/10.1007/s11356-021-13864-z.
Tao, Q., Hou, D.D., Yang, X.E., Li, T.Q., 2016. Oxalate secretion from the root apex of *Sedum alfredii* contributes to hyperaccumulation of Cd. Plant Soil 398, 139–152. https://doi.org/10.1007/s11104-015-2651-x.
Tessier, A., Campbell, P.G.C., Bisson, M., 1979. Sequential extraction procedure for the speciation of particulate trace metals. Anal. Chem. 51 (7), 844–851. https://doi.org/10.1021/ac50043a017.
Wang, Z., Kwon, K.D., Peacock, C., Mo, X.X., Gou, W.X., Feng, X.H., Li, W., 2022. Zn stable isotope fractionation during adsorption onto todorokite: a molecular perspective from X-ray absorption spectroscopy and density functional theory. Geochem. Cosmochim. Acta 327, 116–136. https://doi.org/10.1016/j.gca.2022.04.016.
Wang, Z., Peacock, C., Kwon, K.D., Gu, X.Y., Feng, X.H., Li, W., 2023. Site-specific isotope fractionation during Zn adsorption onto birnessite: insights from X-ray absorption spectroscopy, density functional theory and surface complexation modeling. Geochem. Cosmochim. Acta 348, 68–84. https://doi.org/10.1016/j.gca.2023.03.006.
Wiggenhauser, M., Aucour, A.M., Bureau, S., Campillo, S., Telouk, P., Romani, M., Ma, J.F., Landrot, G., Sarret, G., 2021. Cadmium transfer in contaminated soil-rice systems: insights from solid-state speciation analysis and stable isotope fractionation. Environ. Pollut. 269, 115934. https://doi.org/10.1016/j.envpol.2020.115934.
Wiggenhauser, M., Moore, R.E.T., Wang, P., Bienert, G.P., Laursen, K.H., Blotevogel, S., 2022. Stable isotope fractionation of metals and metalloids in plants: a review. Front. Plant Sci. 13, 840941. https://doi.org/10.3389/fpls.2022.840941.
Wu, L.H., Liu, Y.J., Zhou, S.B., Guo, F.G., Bi, D., Guo, X.H., Baker, A.J.M., Smith, J.A.C., Luo, Y.M., 2013. *Sedum plumbizincicola* X.H. Guo et S.B. Zhou ex L.H. Wu (*Crassulaceae*): a new species from Zhejiang Province, China. Plant Systemat. Evol. 299 (3), 487–498. https://doi.org/10.1007/s00606-012-0738-x.
Wu, L.H., Zhou, J.W., Zhou, T., Li, Z., Jiang, J.P., Zhu, D., Hou, J.Y., Wang, Z.Y., Luo, Y.M., Christie, P., 2018. Estimating cadmium availability to the hyperaccumulator *Sedum plumbizincicola* in a wide range of soil types using a piecewise function. Sci. Total Environ. 637–638, 1342–1350. https://doi.org/10.1016/j.scitotenv.2018.04.386.
Zeng, F.R., Ali, S., Zhang, H.T., Ouyang, Y.N., Qiu, B.Y., Wu, F.B., Zhang, G.P., 2011. The influence of pH and organic matter content in paddy soil on heavy metal availability and their uptake by rice plants. Environ. Pollut. 159, 84–91. https://doi.org/10.1016/j.envpol.2010.09.019.
Zhao, F.J., Ma, Y.B., Zhu, Y.G., Tang, Z., McGrath, S.P., 2015. Soil contamination in China: current status and mitigation strategies. Environ. Sci. Technol. 49, 750–759. https://doi.org/10.1021/es5047099.
Zhao, Y., Li, Y.B., Wiggenhauser, M., Yang, J.L., Sarret, G., Cheng, Q., Liu, J.M., Shi, Y.L., 2021. Theoretical isotope fractionation of cadmium during complexation with organic ligands. Chem. Geol. 571, 120178. https://doi.org/10.1016/j.chemgeo.2021.120178.

Zhong, Q.H., Zhou, Y.C., Tsang, D.C.W., Liu, J., Yang, X., Yin, M.L., Wu, S.J., Wang, J., Xiao, T.F., Zhang, Z.F., 2020. Cadmium isotopes as tracers in environmental studies: a review. Sci. Total Environ. 736, 139585. https://doi.org/10.1016/j.scitotenv.2020.139585.

Zhou, J.W., Li, Z., Liu, M.S., Yu, H.M., Wu, L.H., Huang, F., Luo, Y.M., Christie, P., 2020. Cadmium isotopic fractionation in the soil-plant system during repeated phytoextraction with a cadmium hyperaccumulating plant species. Environ. Sci. Technol. 51 (21), 13598–13609. https://doi.org/10.1021/acs.est.0c03142.

Zhou, J.W., Moore, R., Rehkämper, M., Kreissig, K., Coles, B., Sun, Y.F., Li, Z., Luo, Y.M., Christie, P., Wu, L.H., 2023. Zinc supply affects cadmium uptake and translocation in the hyperaccumulator *Sedum plumbizincicola* as evidenced by isotope fractionation. Environ. Sci. Technol. 57 (14), 5891–5902. https://doi.org/10.1021/acs.est.2c08220.

Zhou, J.W., Moore, R.E.T., Rehkämper, M., Kreissig, K., Coles, B., Wu, L.H., Luo, Y.M., Christie, P., 2024. Cadmium and zinc isotope compositions indicate metal sources and retention mechanisms in different soil particle size fractions. J. Hazard Mater. 461, 132560. https://doi.org/10.1016/j.jhazmat.2023.132560.

Zhou, J.W., Wu, L.H., Zhou, T., Li, Z., Sun, X.Y., Luo, Y.M., Christie, P., 2019. Comparing chemical extraction and a piecewise function with diffusive gradients in thin films for accurate estimation of soil zinc bioavailability to *Sedum plumbizincicola*. Eur. J. Soil Sci. 70, 1141–1152. https://doi.org/10.1111/ejss.12810.

Zhu, C.W., Wen, H.J., Zhang, Y.X., Yin, R.S., Cloquet, C., 2018. Cd isotope fractionation during sulfide mineral weathering in the Fule Zn-Pb-Cd deposit, Yunnan Province, Southwest China. Sci. Total Environ. 616–617, 64–72. https://doi.org/10.1016/j.scitotenv.2017.10.293.